Journal of Low Temperature Physics manuscript No.
(will be inserted by the editor)

E. Zemma · J. Luzuriaga

Turbulent flow around an oscillating body in superfluid helium: dissipation characteristics of the non linear regime.

Received: date / Accepted: date

Abstract By examining the resonance curves of an oscillator submerged in superfluid liquid helium, it is found that their shape is affected by two distinct dissipation regimes when the amplitude is large enough to generate turbulence in the liquid. In a resonance curve, the central part close to resonance, may be in a turbulent regime, but the response is of much lower amplitude away from the resonance frequency, so that the oscillation can still be in the linear regime for frequencies not exactly at resonance. This introduces an ambiguity in estimating the inverse quality factor Q^{-1} of the oscillator. By analyzing experimental data we consider a way of matching the two ways of estimating Q^{-1} and use the information to evaluate the frictional force as a function of velocity in a silicon paddle oscillator generating turbulence in the superfluid.

Keywords Quantum fluids · Turbulence · Superfluid Helium · Non Linear oscillator · Vibrating Paddle · Critical velocity

PACS 67.25.-k , 67.25.dk, 67.25.dg, 47.37.+q

1 Introduction

In Superfluid Turbulence research, one of the experimental methods makes use of oscillators of different shapes submerged in the liquid. Changes in the dissipation of the system are usually taken as an indication of the onset of turbulence. Objects moving in the liquid probe characteristics of turbulence that have a classical analogue and several shapes have been used, such as

E. Zemma
Centro Atómico Bariloche, CNEA, Inst. Balseiro,UNC,CONICET, Argentina
E-mail: zemma@cab.cnea.gov.ar

J. Luzuriaga
Centro Atómico Bariloche, CNEA, Inst. Balseiro,UNC, Argentina

spheres [1–3], quartz tuning forks [4–6] grids [7–11] wires [12–14] and silicon paddles [15]. This method is a part of the wider study of superfluid physics, an active field of research, reviewed in several publications [16–20].

However, in our recent studies [15] we have encountered some discrepancies in the way dissipation is calculated as the fluid enters the turbulent regime and the oscillating systems behaves non linearly.

In the laminar regime the equation of motion corresponds to the well known formula for a forced oscillator with a dissipation term proportional to velocity:

$$m\ddot{x} + \gamma\dot{x} + kx = E_0.cos(\omega t) \tag{1}$$

where x is an angular or linear displacement, m a mass or inertia term, k a generalized spring constant, γ the dissipation term and E_0 is the strength of the excitation. The solution is well known, and for small dissipation, results in a Lorentzian resonance curve. There are two equivalent forms of measuring the dissipation. One can take a resonance curve, plot the amplitude squared, and measure the width of the curve at half the maximum value, Δf. The dissipation Q^{-1},*i.e.* the inverse quality factor, is then

$$Q^{-1} = \Delta f / f_0 \tag{2}$$

with f_0 the resonance frequency.

An equivalent definition makes use of the fact that at resonance the response is enhanced with respect to the static displacement [21] by the factor Q, that is, $A_M = kE_0Q$, or

$$Q^{-1} = \frac{kE_0}{A_M} \tag{3}$$

with A_M the displacement at the maximum of the resonance curve.

In our measurements of a silicon paddle oscillating in superfluid helium [15] both definitions (Eqs. 2 and 3) no longer agree when the oscillator behaves non linearly. Q^{-1} needs to be computed more carefully if one is to obtain a coherent physical picture.

Nonlinear Oscillations have been extensively studied for decades, conceptual treatments and analysis techniques have progressed responding to many problems in the field of experimental physics and engineering [22, 23]. The Duffing equation [23], which for certain parameters presents stable harmonic solutions is a much studied example of non linear variations of Eq. 1. In our oscillator however, nonlinear parameters are not present in the displacement term, but in the velocity. Furthermore, there is also a velocity threshold for turbulence to start. This is an important characteristics of the problem, probably more important than the higher powers in the velocity which also appear. Non linear velocity terms have been studied by Collin *et al* [24] but in their case no threshold appears. Our experimental data show important differences from those reported by Collin *et al* [24] indicating that the experimental systems are not equivalent and require a different analysis. Fincham and Wraight [25] have also considered non linear velocity terms in the low damping limit and we have been able to adapt their approximate method of analysis to our data.

In a submerged oscillator when a threshold critical velocity v_0, is reached turbulence is generated and it is only then that the frictional force F becomes non linear. In their experiments Jager *et al* [1] propose a parabolic shape,

$$F = \beta(v^2 - v_0^2) + \gamma v. \tag{4}$$

In this empirical fit v is the velocity of the oscillating object, β and γ are friction coefficients. Below v_0 the system is linear, that is $F = \gamma v$. Even if the expression is not accurate in all details, the existence of a threshold v_0 is a justified assumption because it reflects the fact that until a certain velocity is surpassed no turbulence is generated. The problem has further complications because once generated turbulence can persist, possibly through several cycles, at lower velocities [1, 4] however as a first approximation we consider a stepwise threshold only. Because of the high proportion of normal fluid in our temperature range, the persistence of the extrinsic generated vorticity, and its corresponding influence in nucleating turbulence [26] below the threshold is expected to be smaller in our experiments. This threshold introduces a new type of non linear behaviour, in addition to the fact that v enters with an exponent which is higher than one.

2 Experimental Results

The experimental setup used has been described elsewhere [15]. A single crystal silicon oscillator with a double paddle of centimeter dimensions oscillates in liquid helium in the 1.55 K to 2.17 K temperature range where the normal fraction is between 14% and 100 % respectively. We report here the data obtained in the Symmetric Torsional (ST) mode, which has a narrow resonance curve around a frequency of 358 Hz inside the liquid. We have calibrated the displacement of this mode so that a signal of 1 mV corresponds to 122 μm, using an interferometric method [15]. The actual displacement however is not a simple traslation, but a rotation, so that at the outer edge of the paddle we estimate that the displacement is 1.6 times and in the inner edge 0.32 times the calibrated value. For simplicity here we report generally values in the laboratory units (mV) directly measured.

In our previous experiment [15] for low amplitudes the resonance curves fit the Lorentzian shape very well. At higher amplitudes, for turbulent flow, the dissipation increases and the resonance curves become wider but can still be fitted reasonably by a Lorentzian. The fit is not so good, but in any case we have associated an inverse quality factor with the width of the curve at half maximum.

In our oscillatory system the velocity is above the threshold only for part of the cycle, as is shown in Fig. 1. This has to be taken into account when analyzing the resonance curves. For small overall dissipation we can assume a sinusoidal oscillation even when the system is turbulent. The relationship between the velocity v and the amplitude A is then $v = A\omega sin(\omega t)$. For the critical threshold values it implies $v_0 = A_C\omega$. In the upper part of Fig. 1 we have represented the velocity of oscillation and v_0. Curve 1 is above the threshold for part of the cycle when $t_1 < t < t_2$ or $t_1 < t < t_2$. The associated

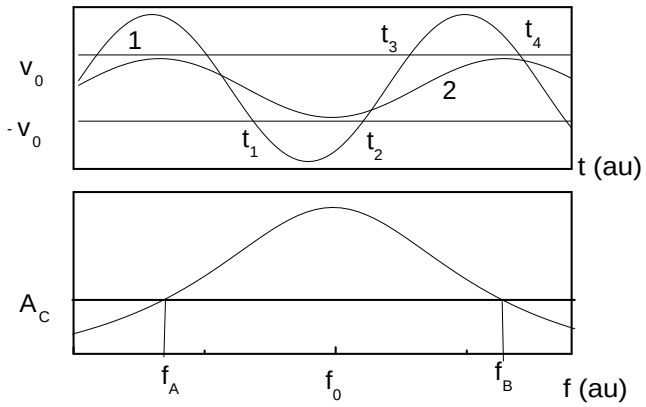

Fig. 1 Oscillation cycle (above) and resonance curve (below) showing the threshold for turbulence. The velocity is above the threshold for times between t_1 and t_2 or t_3 and t_4 (curve 1) and their cyclical equivalents. Outside the central frequency the whole oscillation may be below $v_0 = A_C\omega$ (curve 2 in the figure above) even when it is over A_C in the central part $f_A < f < f_B$

resonance curve is shown in the lower part of Fig. 1. Here it can be seen that when the driving frequency $f < f_A$ or $f > f_B$ the oscillation is always below A_C or v_0 (curve 2 in Fig. 1) and therefore the whole cycle is linear for $f < f_A$ or $f > f_B$.

We have checked this hypothesis using experimental curves from the data of ref. [15]. We have fitted Lorentzian functions for resonance curves using only the points in the region $f < f_A$ or $f > f_B$ where the friction is still linear. The data are shown in Fig. 2 where the points selected are shown as closed symbols, and the fitted curves as dotted lines. Because the original experimental data were taken over a relatively narrow window, we have been forced to overestimate the experimental value of A_C for the higher amplitude curves, changing the boundary frequencies f_A and f_B. However, the qualitative behavior observed appears to be robust with respect to the actual value of A_C. In the central part of the data $f_A < f < f_B$ the interpolation is well above the experimental points, in open symbols. In this region the amplitude of oscillation is above A_C and the friction is non linear. The curves with higher excitation amplitude show larger deviations as can be expected because $A > A_C$ for a larger section of the oscillation.

A Lorentzian fit of the whole curve has also been tried, and the overall fit is fair, as can be seen in the full line in Fig. 2. But looking in more detail it can be seen that there is a slight assymetry in the experimental points, and the tails are not so well adjusted by the Lorentzian curve. This is illustrated in the lower part of Fig. 2, where we show the deviations of the experimental points from the two fits. The closed symbols correspond to a fit in the region $f < f_A$ or $f > f_B$ and the open symbols to a fit of all the experimental data. It can be seen that the spread is greater for the open symbols, and also

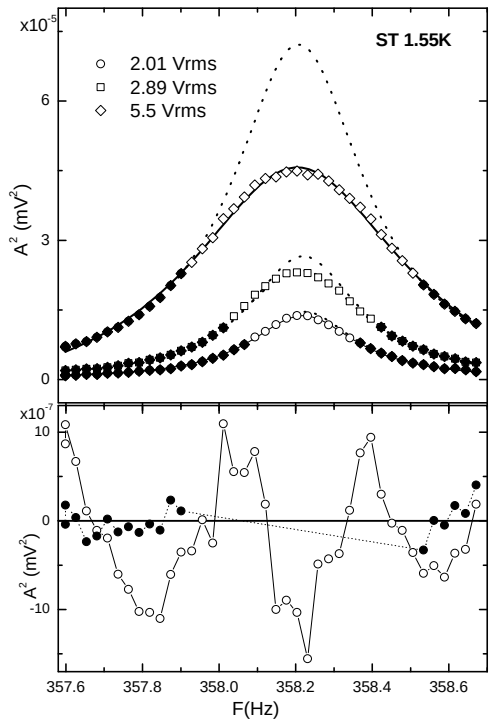

Fig. 2 Above: Resonance curves at 1.55 K for different excitation amplitudes for the ST mode of an oscillating silicon paddle [15]. Open symbols: all experimental points, closed symbols: points estimated to be below the threshold. In dotted lines we plot Lorentzian fits to the points below threshold only and in full lines fits to the whole curve for the higher amplitude of excitation. Below: Distance between the two fits and the experimental points in the higher excitation curve. Open symbols: fit over the whole curve, closed symbols: fit of the tail region only.

that the distribution is not at random but alternates between positive and negative values of the distance from the fitted curve.

Fig. 3 shows the width of the curves Δf (lower panel) calculated using the whole curve fit in open symbols and that using only the tails ($f < f_A$ or $f > f_B$) in closed symbols, as a function of the amplitude at resonance. It can be seen that the closed symbols almost coincide in magnitude with those of the low amplitude, laminar regime. We attribute the small deviations to experimental error in determining f_A and f_B. The coincidence is due to the fact that the Lorentzians are fitted to the tails only, a region still laminar and therefore the dissipation is the same that for the rest of the laminar regime. On the other hand, the open symbols show an increase in Δf due to the turbulent part of the cycle. In the upper panel we show a similar effect when plotting the excitation voltage against the amplitude. In this graph the laminar regime appears as a linear relation between the amplitude

and excitation. As above, closed symbols correspond to the tails, and are almost linear up to the higher values of excitation, while the open symbols curve upwards. The threshold amplitude A_C is defined as the point where the plateau ends (lower graph, open simbols) and it coincides with the amplitude where the relation between excitation and amplitude stop being linear (upper graph).

The above observations imply that the resonance curves are influenced by two different dissipation mechanisms, one linear for points such that $f < f_A$ or $f > f_B$ and one with non linear terms for the central, high amplitude part of the curve.

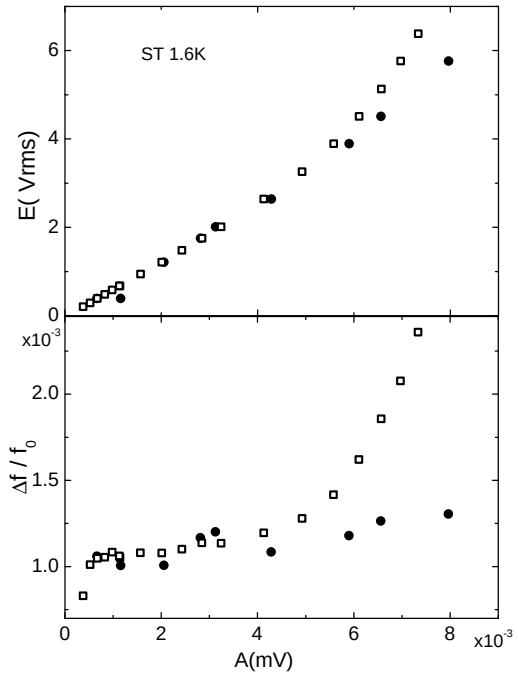

Fig. 3 Excitation voltage (above) and width of resonance curves (below) as a function of the response amplitude. The open symbols are taken from the whole resonance curve, and the closed symbols to magnitudes extracted from fits to the tails of the resonance curves where we estimate that the system is linear. The closed symbols are closer to a straight line in the upper graph or a plateau in the lower.

This presents a problem for the definition of Q^{-1} from Eq. 2 because the Lorentzian fit is forced on a curve which is not wholly Lorentzian. The other definition, Eq. 3 is perhaps more directly related to the turbulent state because it is associated with the energy dissipation at the maximum, where turbulence effects are stronger.

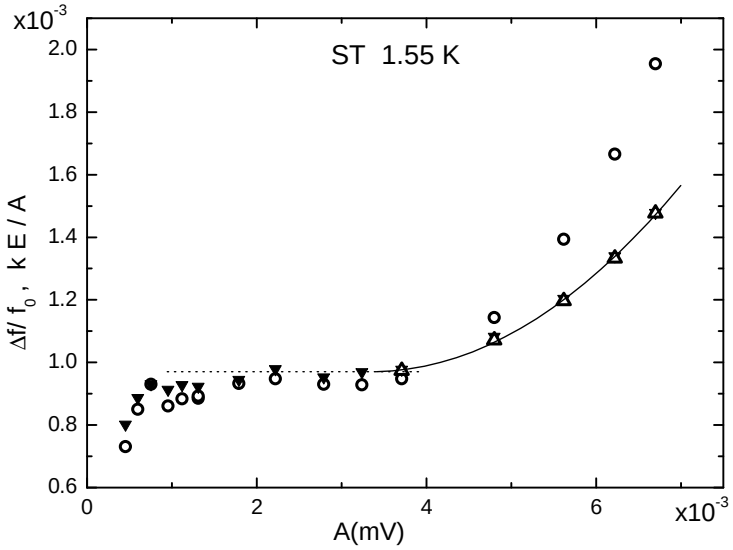

Fig. 4 Comparison of the definitions of Q^{-1} given by equations 2 and 3. Open circles: $\Delta f/f_0$ (Eq. 2), closed inverted triangles: Excitation divided by amplitude (Eq. 3) scaled to coincide in the plateau of the linear region, open upright triangles: $\Delta f/f_0$ in the non linear region scaled by a constant factor ≈ 0.5. The full line is a quadratic fit to the non linear region.

In any case, the definitions are no longer equivalent, as we show in Fig. 4. Here we have plotted Q^{-1} derived from Eq. 2 and $\Delta f/f_0$ against the amplitude at resonance, and on the same graph the values of excitation divided by the amplitude and multiplied by an adjustable constant as would correspond to Q^{-1} defined through Eq. 3. The constant has been chosen so that both values coincide in the low amplitude part of the curves, *i.e.* the laminar regime. For high values of amplitude both data set deviate from a constant but they do not coincide showing that in the turbulent regime the two definitions of Q^{-1} are no longer equivalent. However, correcting the increase of the width of of resonance curve by a factor of about one half, the data agree with those of Eq. 3 as can be seen in the upright open triangles in Fig. 4. The data above the constant plateau can also be fitted very well by a quadratic expression, shown as a full line in the figure. The non linear fit is valid for amplitudes above A_C and merges with the plateau with zero slope, as could be expected for an extra dissipation that is absent for lower amplitudes.

3 Discussion

The Q^{-1} factor in an oscillator can be also calculated theoretically by finding the energy loss over a cycle, and dividing it by the the total energy of the oscillator. In a system with small losses, the energy dissipated can be obtained using the principle of energy balance [21, 25]. We assume the movement is close to sinusoidal, $x = Asin(\omega t)$, $v = \omega Acos(\omega t)$ and we propose a frictional force that is cubic in the velocity and has a threshold v_0 for the non linear term.

$$F_{NL} = \epsilon(v - v_0)^2 v = \epsilon(\omega Acos(\omega t) - v_0)^2 \omega Acos(wt) \tag{5}$$

adding the linear term $F_L = \gamma v = \gamma \omega Acos(\omega t)$ and integrating over a cycle, the energy dissipated ΔE is

$$\Delta E = \int_0^{2\pi\omega} \gamma\omega^2 A^2 cos^2(\omega t)\, dt$$

$$+2\int_{t_1}^{\pi/\omega - t_1} \epsilon\omega^2 A^2 cos^2(\omega t)\left(\omega Acos(\omega t) - v_0\right)^2 dt. \tag{6}$$

The limits of integration of the non linear part $t_1 = (1/\omega)arcsin(\frac{Ac}{A})$ and $t_2 = \pi/\omega - t_1$ are indicated in Fig. 1 and we have used the symmetry of the sine function. Performing the integration we obtain

$$\begin{aligned}\Delta E = {} & A^2\pi\gamma\omega \\ & -1/8A^4\epsilon\omega^3\left[-6\pi + 8sin(2\omega t_1) + sin(4\omega t_1) + 12\omega t_1\right] \\ & -A^2\epsilon\omega v_0^2\left[-\pi + sin(2\omega t_1) + 2\omega t_1\right].\end{aligned} \tag{7}$$

To find Q^{-1} we have to divide ΔE by the energy stored in the spring at the maximum displacement, $E = 1/2kA^2$. Then Eq. 7 gives a constant Q^{-1} for low amplitudes and a quadratic expression for $A > A_C$. Thus the model reproduces the functional dependence seen in the experimental data for both the Q^{-1} definitions considered since they basically differ by a constant factor. The threshold terms do not affect significantly the amplitude behaviour being included in the slowly changing term t_1. As discussed by Pippard [21] a frictional force with a given velocity exponent ν implies a variation of Q^{-1} with an exponent $\nu - 1$. Thus it appears that the threshold term affects the resonance curves more than the exponent of the friction dependence on velocity (or amplitude).

We have further analyzed the data obtained previously and already partially reported [15], with the above considerations in mind. In Fig. 5 (upper panel) we plot the excitation against velocity for different temperatures. The velocity has been calibrated as described previously [15], and it is proportional to the amplitude at resonance. The slopes of the linear part follow the same function of temperature as the plateau seen in Q^{-1}, as expected for the linear system described by Eq. 1. The non linear part has been fitted by a cubic expression, shown as full lines in the figure. If we assume, as done by Jager *et al* [1] that by considerations of energy balance [21, 25] we can identify the velocity dependence of the excitation with that of the frictional force, the data show a cubic frictional force for our paddle also consistent with

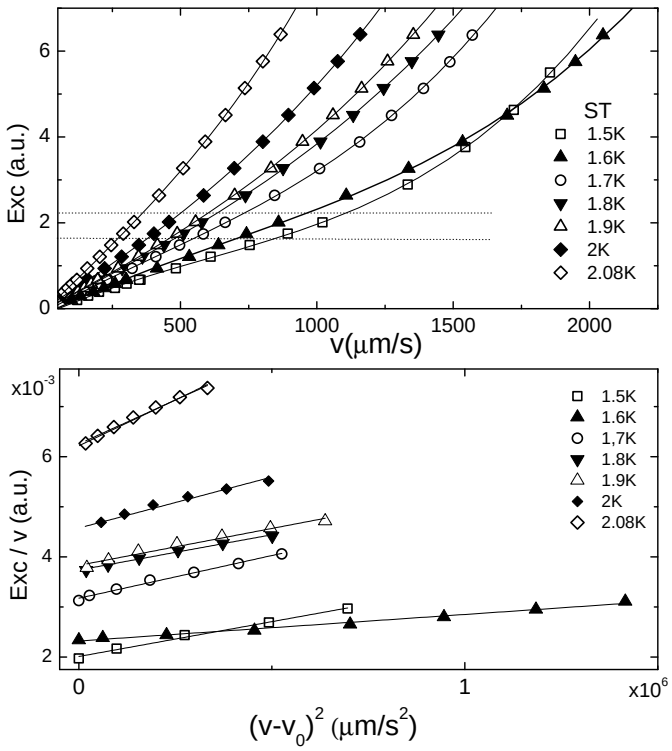

Fig. 5 Excitation plotted against velocity for different temperatures. The lines are fits to a cubic expression. The relation between amplitude of oscillation and velocity has been calibrated [15] and corresponds to 2.7 μm/s per mV.

the quadratic Q^{-1} dependence and Eq. 7. In the lower panel of Fig. 5 we show the same data with a different scaling which emphasizes the functional dependence proposed. In the ordinate axis we plot the excitation divided by the velocity (Exc/v) for points above the threshold and in the abscissa axis the velocity minus the threshold velocity squared ($(v - v_0)^2$) for different temperatures. As expected from the functional dependence proposed in Eq. 5 the plots are straight lines and the points where they cut the $y-$axis are higher for higher temperatures, corresponding to the higher slopes of the Exc *vs* v curves. We have also tried quadratic fits for the excitation *vs* velocity curves but they are poor, so we conclude that our paddle shows a different behaviour than the sphere of reference [1].

A so far unexplained feature of these plots is that the excitation corresponding to the change in regime is approximately the same for all the temperatures measured even when the critical velocity or amplitude changes with temperature. This is shown by dotted lines in Fig. 5 upper panel, placed

at the approximate excitation limits in which the system enters the non linear regime. The critical velocity measured increases with decreasing temperature while the slope of the linear part decreases and it appears that the two effects compensate in some way so that we need to supply a level of excitation which is relatively constant to observe the onset of turbulence.

4 Conclusions

We have shown that the resonance curves in an oscillator moving in superfluid helium have a double structure, because away from the maximum the fluid motion can be laminar, while it can be turbulent close to the maximum.

The resulting difficulty in defining a quality factor has been resolved empirically by re normalizing the definition of Eq. 2 and by considering energy balance in our paddle we find that the force in the damping is fitted by a cubic polynomial, with a threshold velocity.

5 Acknowledgments

We wish to thank A. Badía Majós for fruitful discussions. This work was partially supported by grant PICT00-03-08937 from ANPCyT, Argentina and 06/C252 grant from U.N. Cuyo.

References

1. J. Jäger, B. Schuderer, and W. Schoepe, *Phys. Rev. Lett.*, **74**, 566 (1995).
2. J. Luzuriaga, *J. Low Temp. Phys.*, **108**, 267 (1997).
3. W. Schoepe,*J. Low Temp. Phys.* ,**150**,724 (2008).
4. M. Blažková, D. Schmoranzer, L. Skrbek, and W. F. Vinen, *Phys. Rev. B*, **79**,054522(2009).
5. M. Blažková, M. Clovecko, E. Gao, L. Skrbek, and P. Skyba, *J. Low Temp. Phys.*, **148**,305 (2007).
6. M. Blažková, T. Chagovets, M. Rotter, D. Schmoranzer, and L. Skrbek, *J. Low Temp. Phys.*, **150**, 194 (2008).
7. W. F. Vinen, L. Skrbek, and H. A. Nichol, *J. Low Temp. Phys.*,**135**(5-6),423 (2004).
8. H. A. Nichol, L. Skrbek, P. C. Hendry, and P. V. E. McClintock, *Phys. Rev. Lett.*,**92**, 244501 (2004).
9. H. A. Nichol, L. Skrbek, P. C. Hendry, and P. V. E. McClintock, *Phys. Rev. E*, **70**, 056307 (2004).
10. D. Charalambous, L. Skrbek, P. C. Hendry, P. V. E. McClintock, and W. F. Vinen, *Phys. Rev. E*,**74**,036307 (2006).
11. V. Efimov, D. Garg, M. Giltrow, P. McClintock, L. Skrbek, and W. Vinen, *Journal of Low Temperature Physics*, **158**,462 (2010).
12. H. Yano, A. Handa, H. Nakagawa, M. Nakagawa, K. Obara, O. Ishikawa, and T. Hata, *J. of Phys. Chem. Solids*, **66**(8-9),1501 (2005).
13. H. Yano, N. Hashimoto, A. Handa, M. Nakagawa, K. Obara, O. Ishikawa, and T. Hata, *Phys. Rev. B* ,**75**,012502 (2007).
14. H. Yano, Y. Nago, R. Goto, K. Obara, O. Ishikawa, and T. Hata, *Phys. Rev. B*, **81**,
220507 (2010).

15. E. Zemma and J. Luzuriaga, *Journal of Low Temperature Physics*, **166**,171 (2012).
16. J. Tough, "Chapter 3: Superfluid turbulence," in *Progress in Low Temperature Physics* (D. Brewer, ed.), vol. 8 of *Progress in Low Temperature Physics*, pp. 133 – 219, Elsevier, 1982.
17. R. J. Donnelly and C. E. Swanson, *Journal of Fluid Mechanics*, **173**, 387(1986).
18. R. J. Donnelly, *Physica B: Condensed Matter*, **329**, 1 (2003). Proceedings of the 23rd International Conference on Low Temperature Physics.
19. W. F. Vinen, *J. Low Temp. Phys.*, **145**, 7 (2006).
20. W. F. Vinen, *Phil. Trans. Roy. Soc.*, **366**, 2925 (2008).
21. A. B. Pippard, *The physics of vibration. Vol.1: The simple classical vibrator.* Cambridge: University Press, 1978.
22. W. Weaver, S. Timoshenko, and D. Young, *Vibration problems in engineering.* Wiley-Interscience, 1990.
23. A. H. Nayfeh and D. T. Mook, *Nonlinear Oscillations.* Wiley & Sons, New York, 1979.
24. E. Collin, Y. M. Bunkov, and H. Godfrin, *Phys. Rev. B*, **82**, 235416 (2010).
25. D. G. Fincham and P. C. Wraight, *Journal of Physics A: General Physics*, **5**(2), 248 (1972).
26. R. Hänninen, M. Tsubota, and W. F. Vinen, *Phys. Rev. B*, **75**, 064502 (2007).